Supporting information
:supplementary figure 1-18 and table 1-2

Ribophorin-2 regulates breast tumor initiation and metastasis through the functional suppression of GSK3β

Ryou-u Takahashi[1], Fumitaka Takeshita[1], Kimi Honma[1], Masaya Ono[2], Kikuya Kato[3] & Takahiro Ochiya[1*]

*Address correspondence to Takahiro Ochiya, Ph.D.
Chief, Division of Molecular and Cellular Medicine,
National Cancer Center Research Institute,
1-1, Tsukiji 5-chome, Chuo-ku, Tokyo 104-0045, Japan
Phone: +81-3-3542-2511 ext. 4800
Fax: +81-3-5565-0727
E-mail: tochiya@ncc.go.jp

1) Division of Molecular and Cellular Medicine,
2) Division of Chemotherapy and Clinical Research, National Cancer Center Research Institute, 1-1, Tsukiji 5-chome, Chuo-ku, Tokyo 104-0045, Japan
3) Research Institute, Osaka Medical Center for Cancer and Cardiovascular Diseases, 1-3-2 Nakamichi, Higashinari-ku, Osaka 537-8511, Japan.

Running Title: RPN2 stabilizes p53 mutant in breast cancer
Keywords: Breast cancer, Cancer stem cell, Mutant p53, GSK3β, Heat shock proteins

A

Fat Pad Injection with CSCs
Cell line: MDA-MB-231-D3H2-LN-Luc (MM231-LN)
Day 18

Cell Number (cells/site)	10^2	10^3	10^4	*Unsorted cells 10^6
Tumor Formation	3/4	3/4	4/4	2/2

*Unsorted cells as positive control

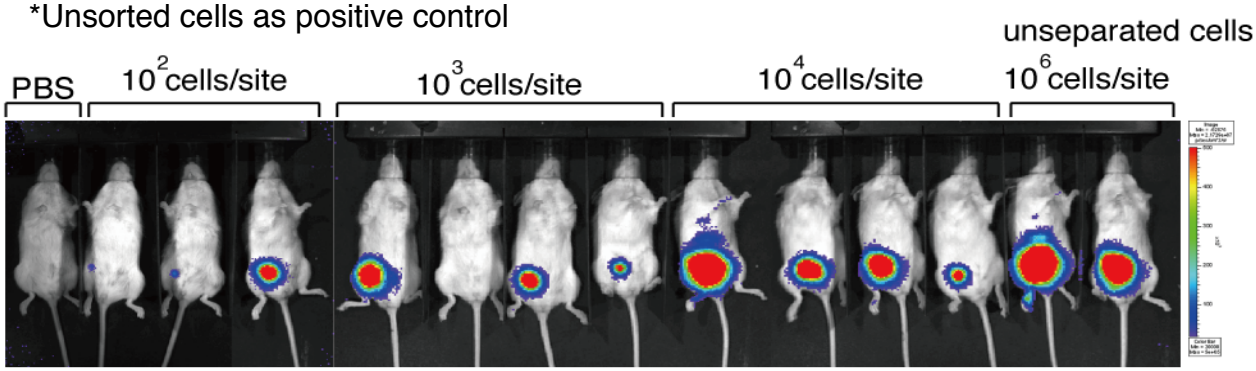

B

Fat Pad Injection with CSCs
Cell line: MM231-LN

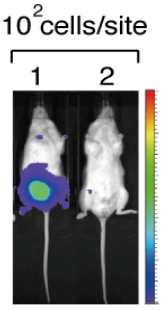

Day 42	CSCs	Non-CSCs
Tumor Formation	3/3	1/3

1. CSCs Fraction
2. Unseparated Fraction

Figure S1

Limiting Dilution Analysis of Breast CSC Fraction.

(A) Tumor incidence of CSCs ($CD44^{high}/CD24^{low}$) after mammary fat pad injection.

(B) Tumor incidence of CSCs and non-CSCs after mammary fat pad injection.

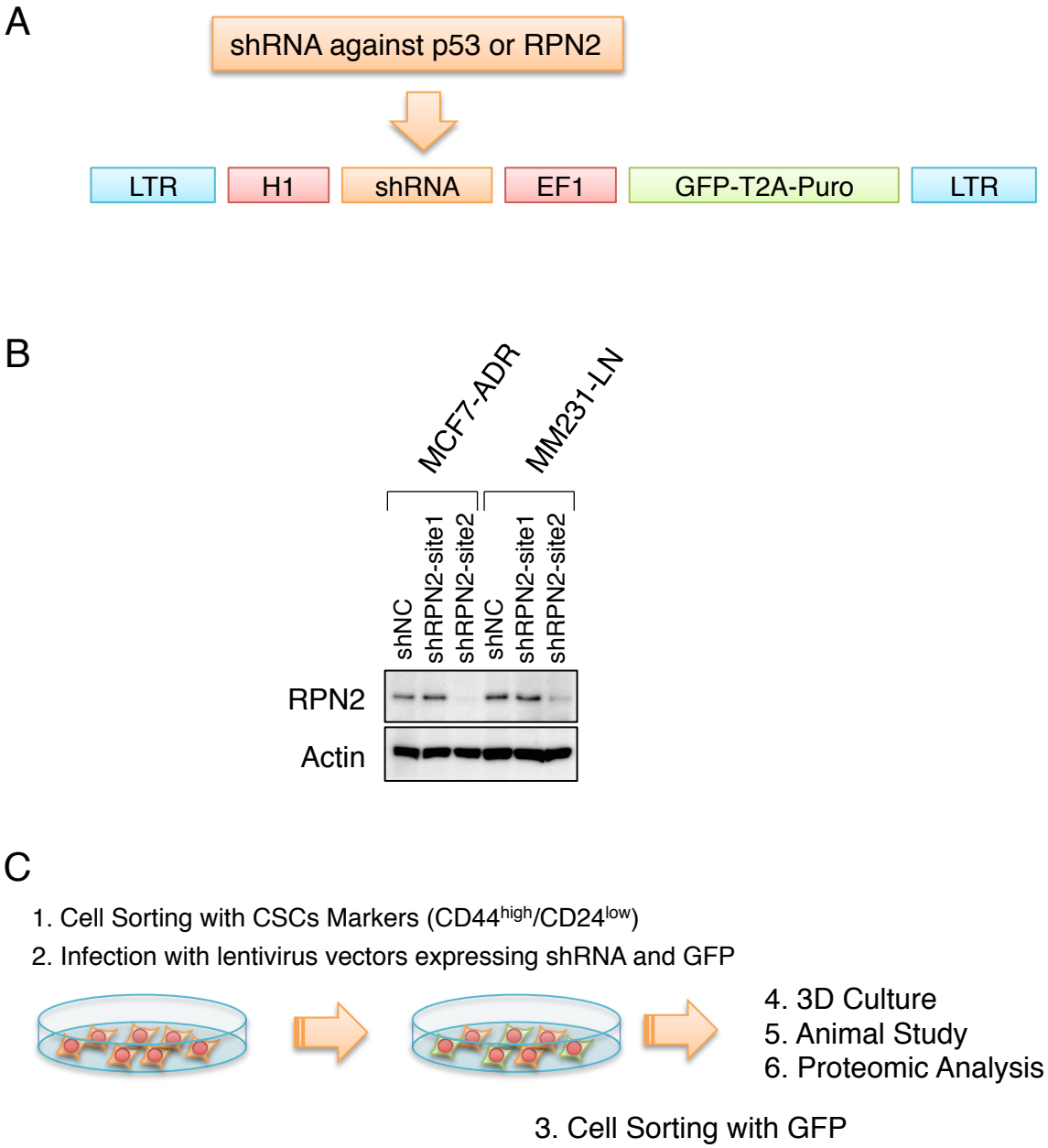

Figure S2

Lentiviral vectors utilized in the present study.

(A) Diagram of the lentiviral vector. The characterization of the knockdown effect of pGreenpuro-RPN2shRNA (B) by Western blotting. (C) Experimental procedure for the analysis of RPN2 in CSCs fraction.

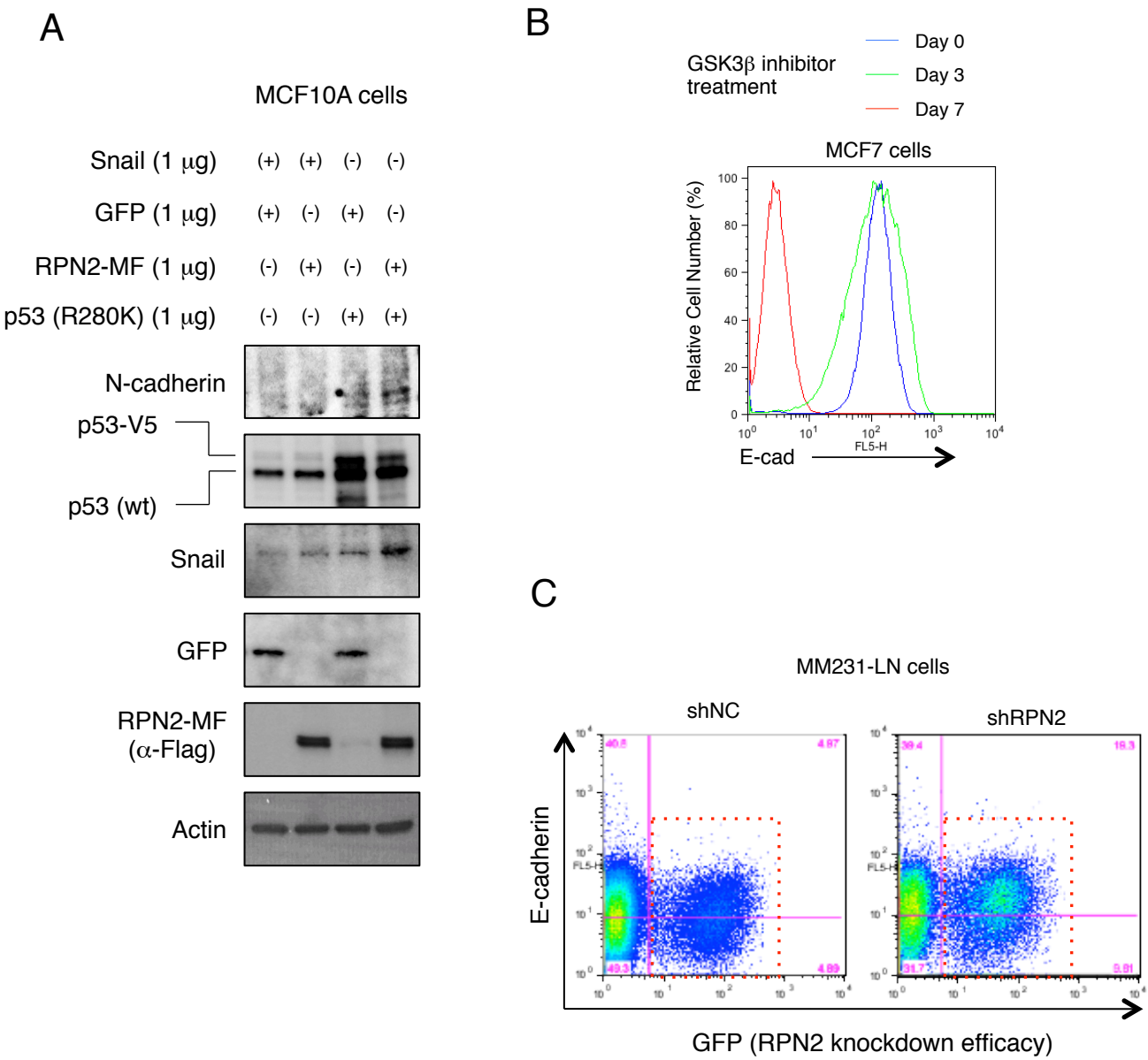

Figure S3

(A) Western blot analysis. Cell lysates were subjected to western blot analysis with anti-p53, anti-Flag, anti-Snail, anti-N-cadherin, anti-GFP and anti-actin antibodies. (B) GSK3β inhibitor (CHIR99021, 3 μM) suppressed E-cadherin expression. (C) RPN2 knockdown reduced E-cadherin negative fraction.

A

NOD-Scid mice, Female, 6 week-old

Subcutaneous Injection of CSC

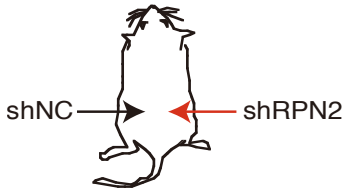

Cell line	Cell umber (cells/site)	shRPN2	shNC
MM231-LN	10^2	1/5	5/5

Day 55

Luciferase

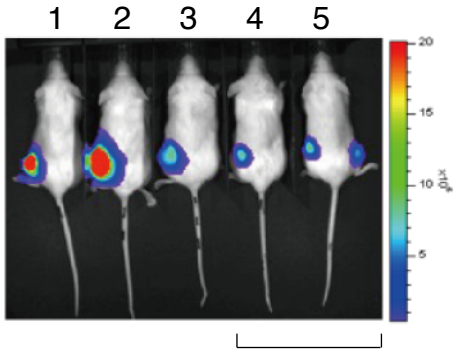

B

NOD-Scid mice, Female, 6 week-old

Subcutaneous Injection of CSC

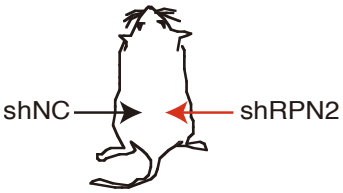

Day 70

Luciferase

GFP

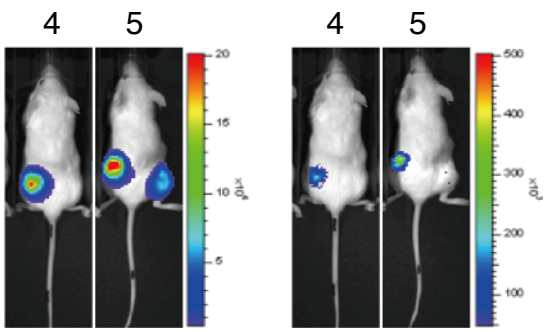

Figure S4

RPN2 regulates the tumorigenicity of CSCs.

(A) Tumor incidence of CSCs ($CD44^{high}/CD24^{low}/GFP^{high}$) in MM231-LN shNC (Left) and MM231-LN shRPN2 (Right) cells after subcutaneous injection.

(B) Monitoring the knockdown efficacy of RPN2 by GFP expression.

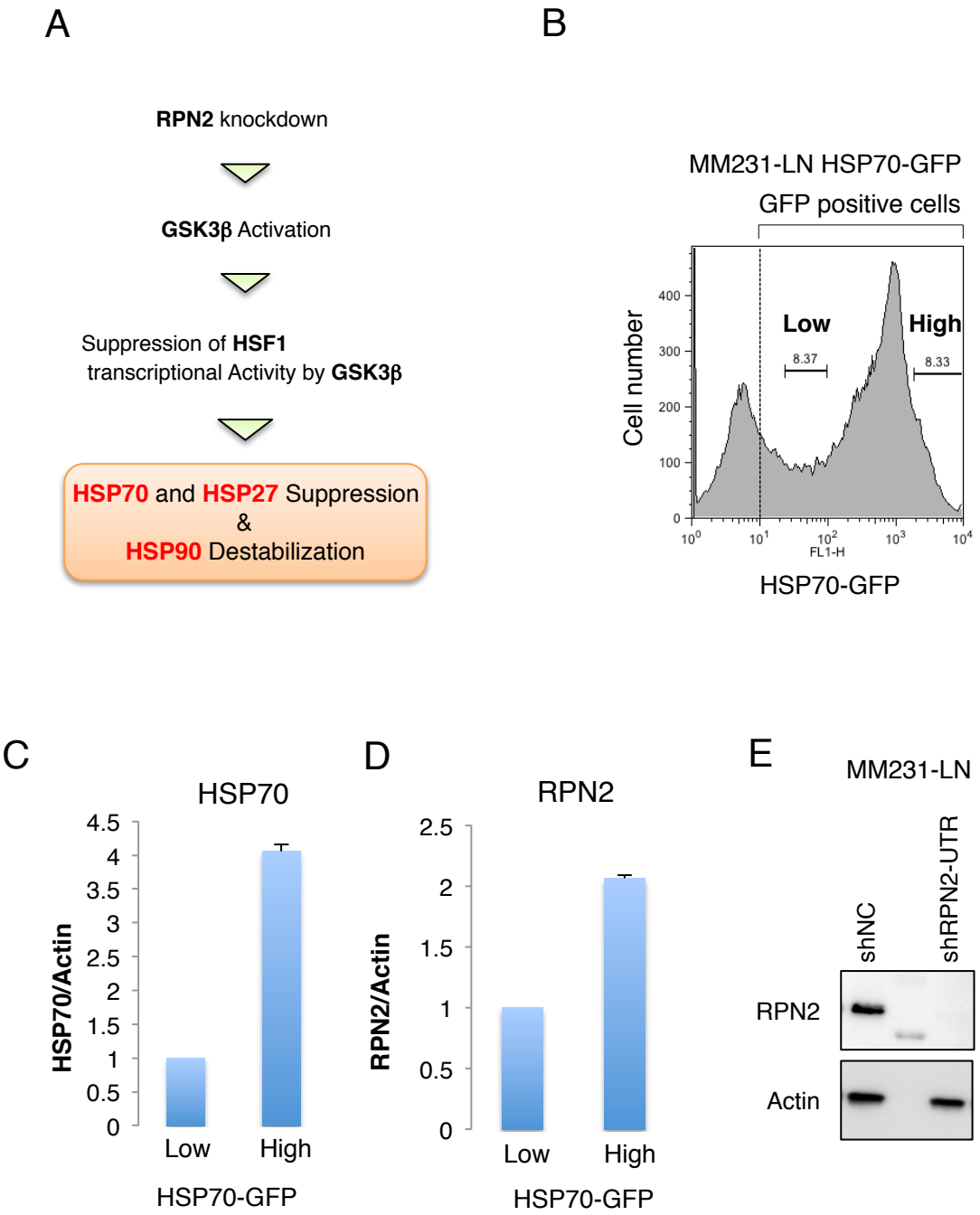

Figure S5

GSK3β-mediated downregulation of heat shock proteins in RPN2 knockdown cells.

(A) Working model for GSK3β-mediated downregulation of heat shock proteins in RPN2 knockdown cells. (B) Establishment of MM231-LN cells expressing HSP70 promoter driven GFP (MM231-LN HSP70-GFP). (C) and (D) MM231-LN HSP70-GFP cells were segregated by cell sorting into GFP high and GFP low subsets as in (B); sorted subsets were then compared for HSP70 and RPN2 expression by quantitative real-time PCR. (E) Establishment of MM231-LN shRPN2-UTR. Western blot analysis was performed with anti-RPN2 and anti-Actin antibodies.

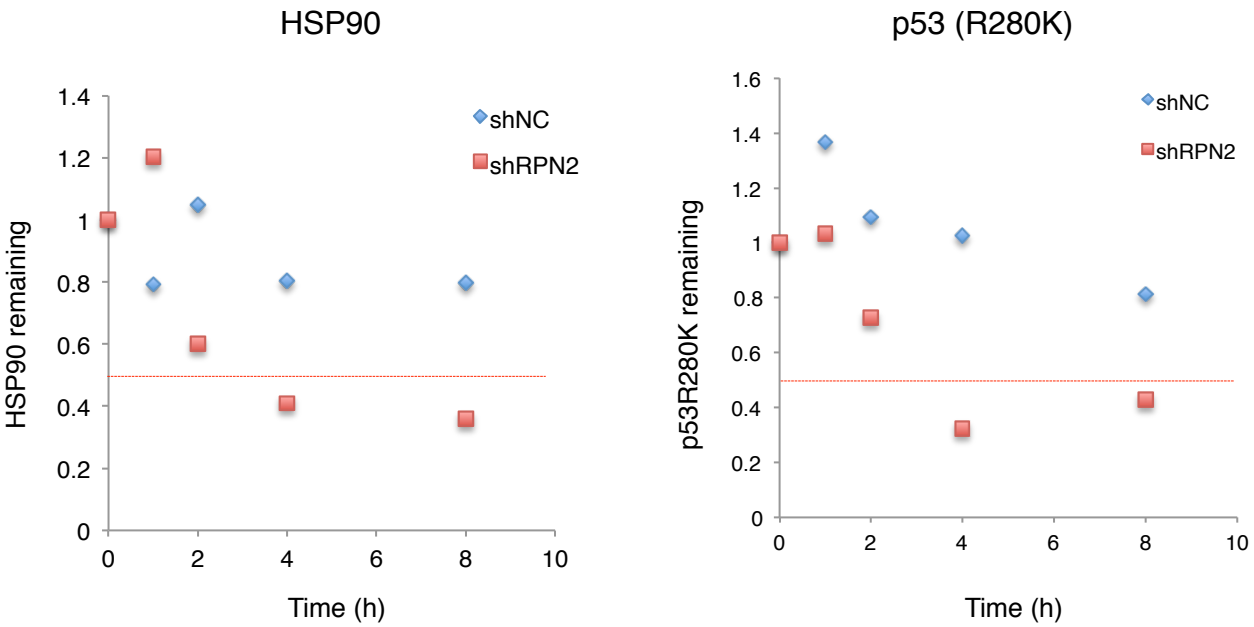

Figure S6
RPN2 knockdown reduced half-life of HSP90 and p53R280K.
(A) MM231-LN shNC and MM231-LN shRPN2 cells were treated with cycloheximide (50 µg/ml) for 0–8 h. Cell lysates were subjected to western blotting with anti-HSP90, anti-p53 and anti anti-actin antibodies (fig. 5a and 6e). Half-life of HSP90 and p53R280K were calculated from the western blots (signal intensity was normalized to beta-actin).

A

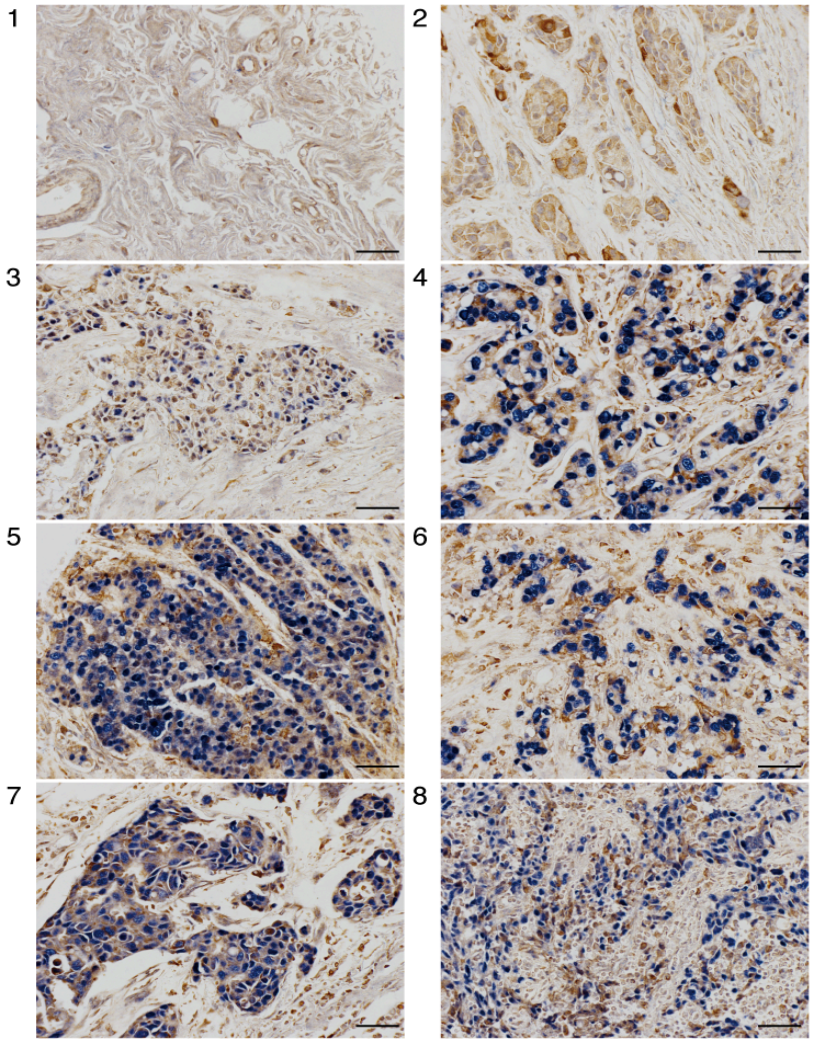

B

Sample Number	Age	Sex	Diagnosis	T stage	LN	ER	PR
1	37	F	Normal	-	-	-	-
2	39	F	Infiltrating ductal carcinoma	T3	0/37	(-)	(-)
3	65	F	Infiltrating ductal carcinoma	T2	0/9	(+)	(-)
4	33	F	Infiltrating ductal carcinoma	T3	25/25	(+)	(+)
5	43	F	Infiltrating ductal carcinoma	T3	25/25	(-)	(-)
6	35	F	Infiltrating ductal carcinoma	T3	8/14	(+)	(-)
7	47	F	Infiltrating ductal carcinoma	T2	8/17	(-)	(-)
8	45	F	metastatic carcinoma in lymph node	T1c	22/26	(-)	(-)

Figure S7

The expression of RPN2 and mutant p53 in breast cancer tissues. (*A*) Immunohistochemical staining of RPN2 (Brown) and mutant p53 (Blue) in breast cancer tissues classified by the extent of lymph node metastasis (LN) as shown in (*B*). ER, Estrogen Receptor; PR, Progesterone Receptor. Scale bar, 50 μm.

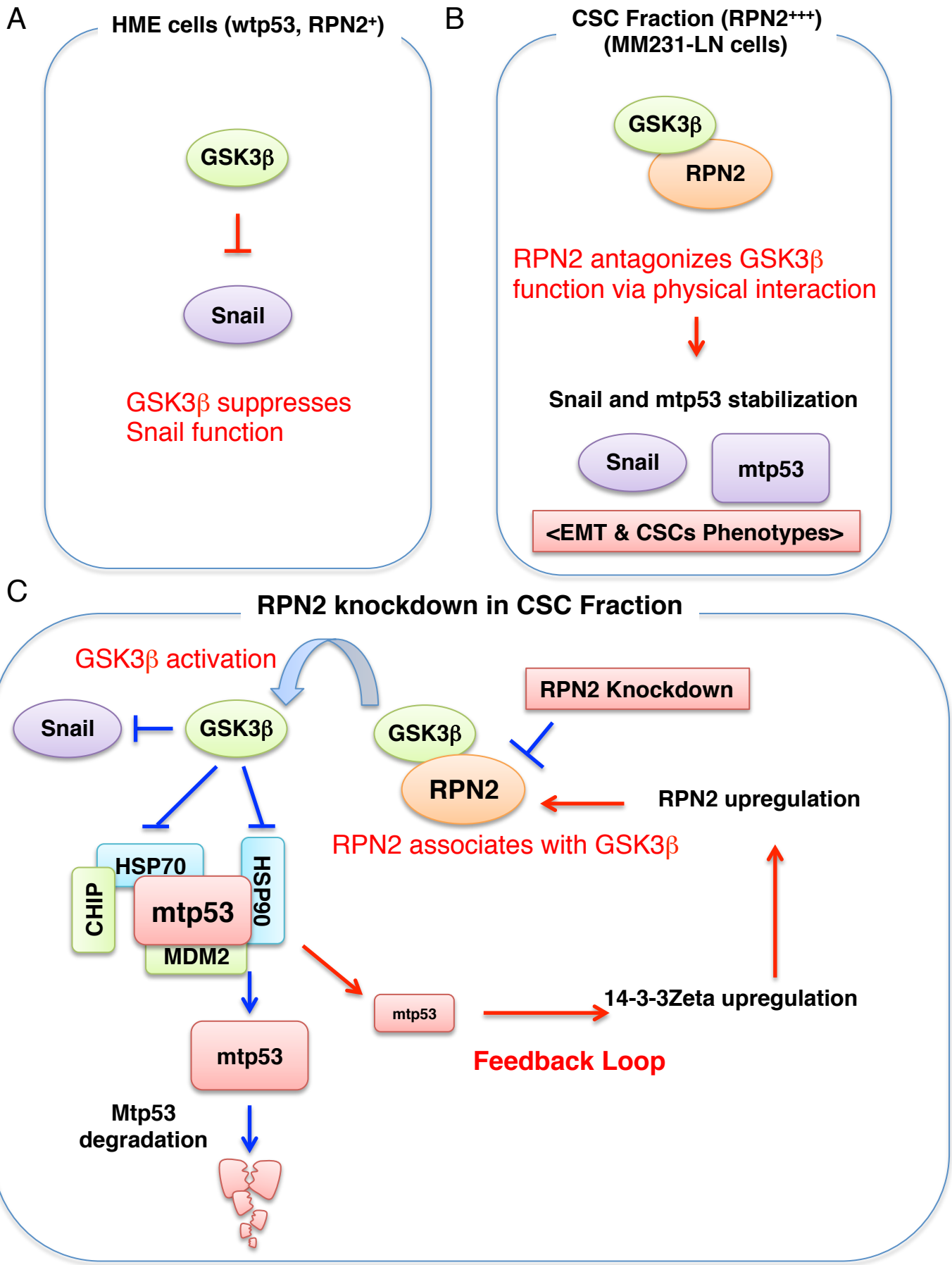

Figure S8 Working model for RPN2 mediated mtp53 stabilization.

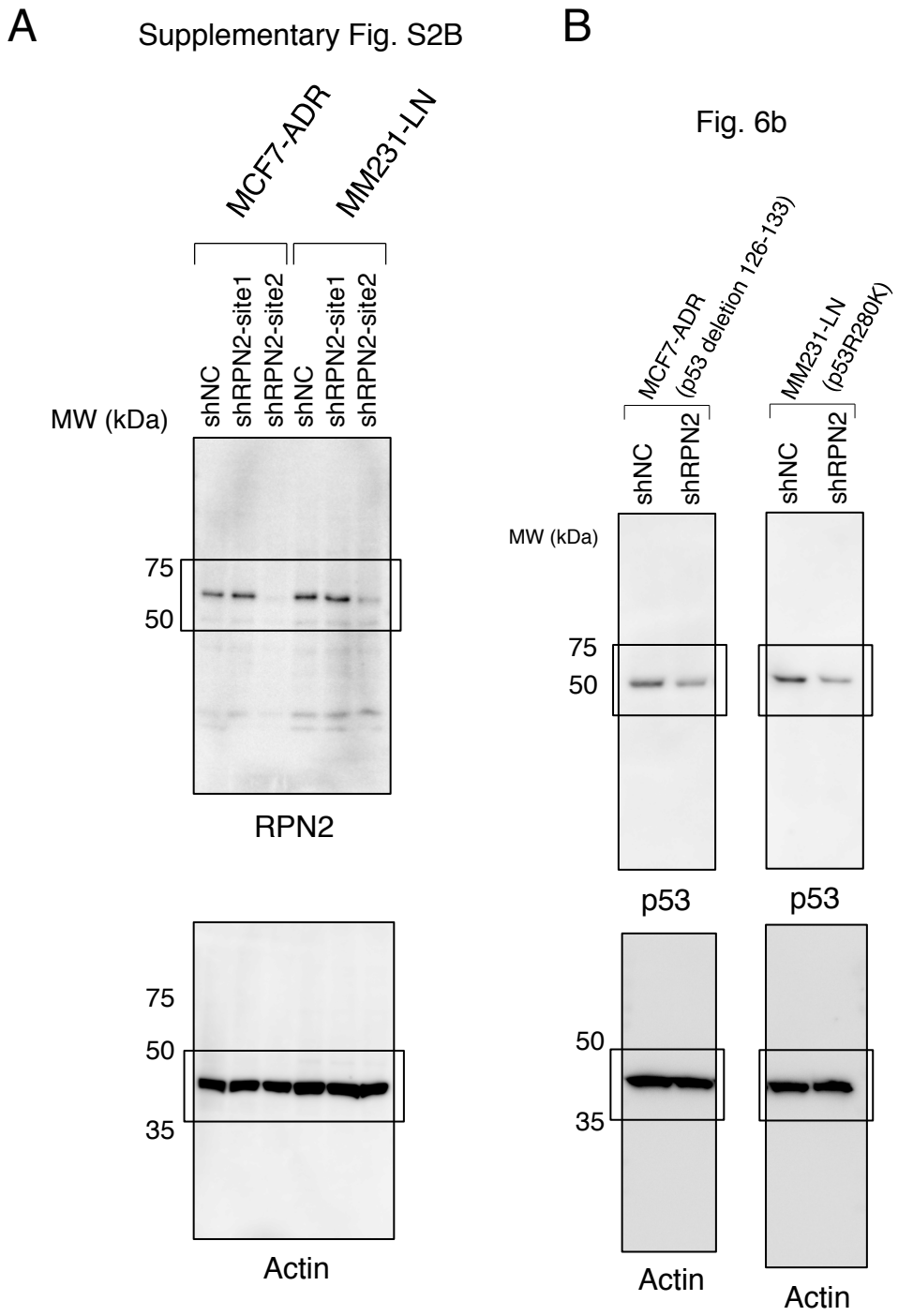

Figure S9 Full scans of western blots shown in the main and supplementary figures. (A) The full blots shown in Fig. S2B with the locations of MW (molecular weight). (B) The full blots shown in Fig. 6b.

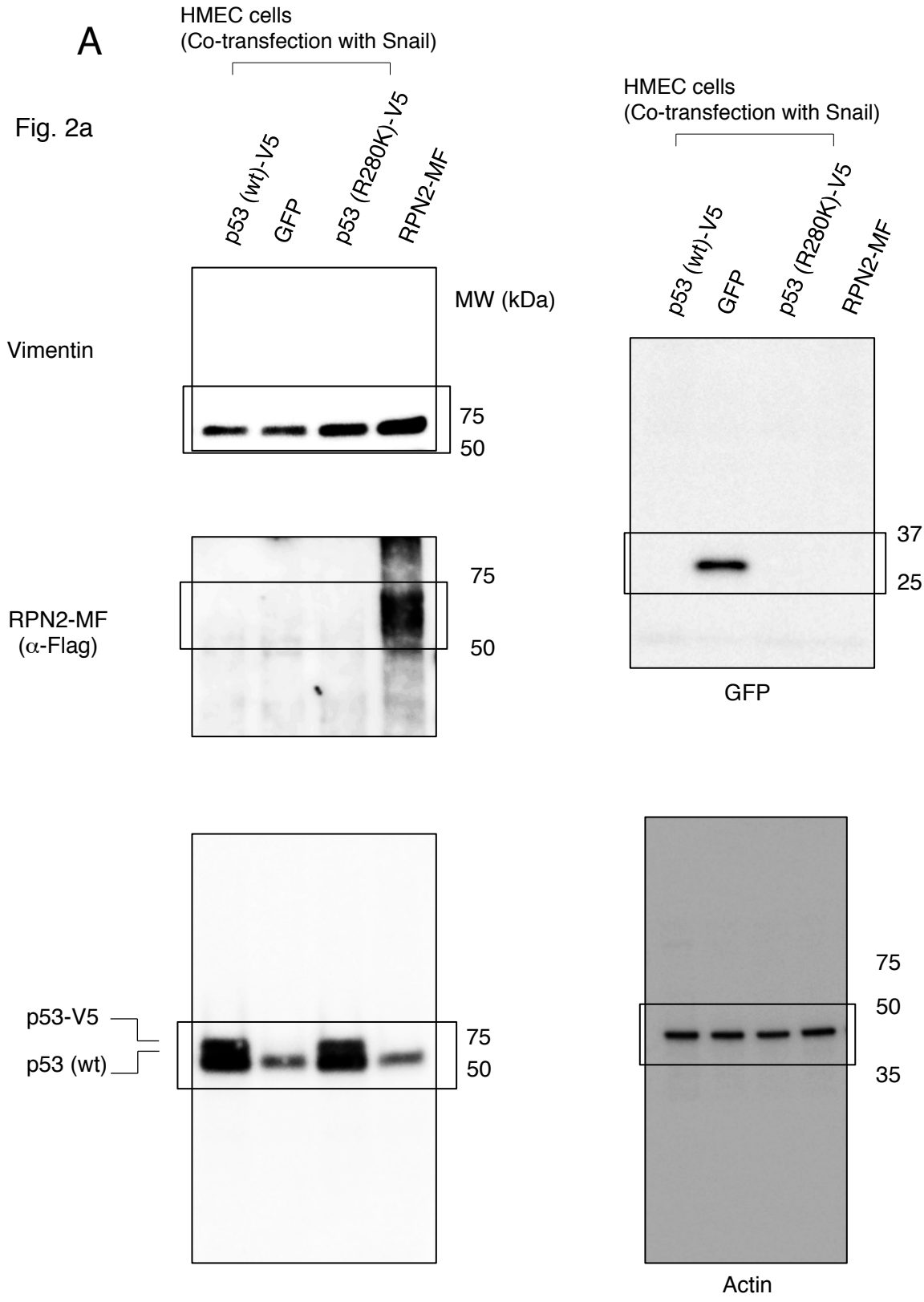

Figure S10 Full scans of western blots shown in the main and supplementary figures. (A) The full blots shown in Fig. 2a.

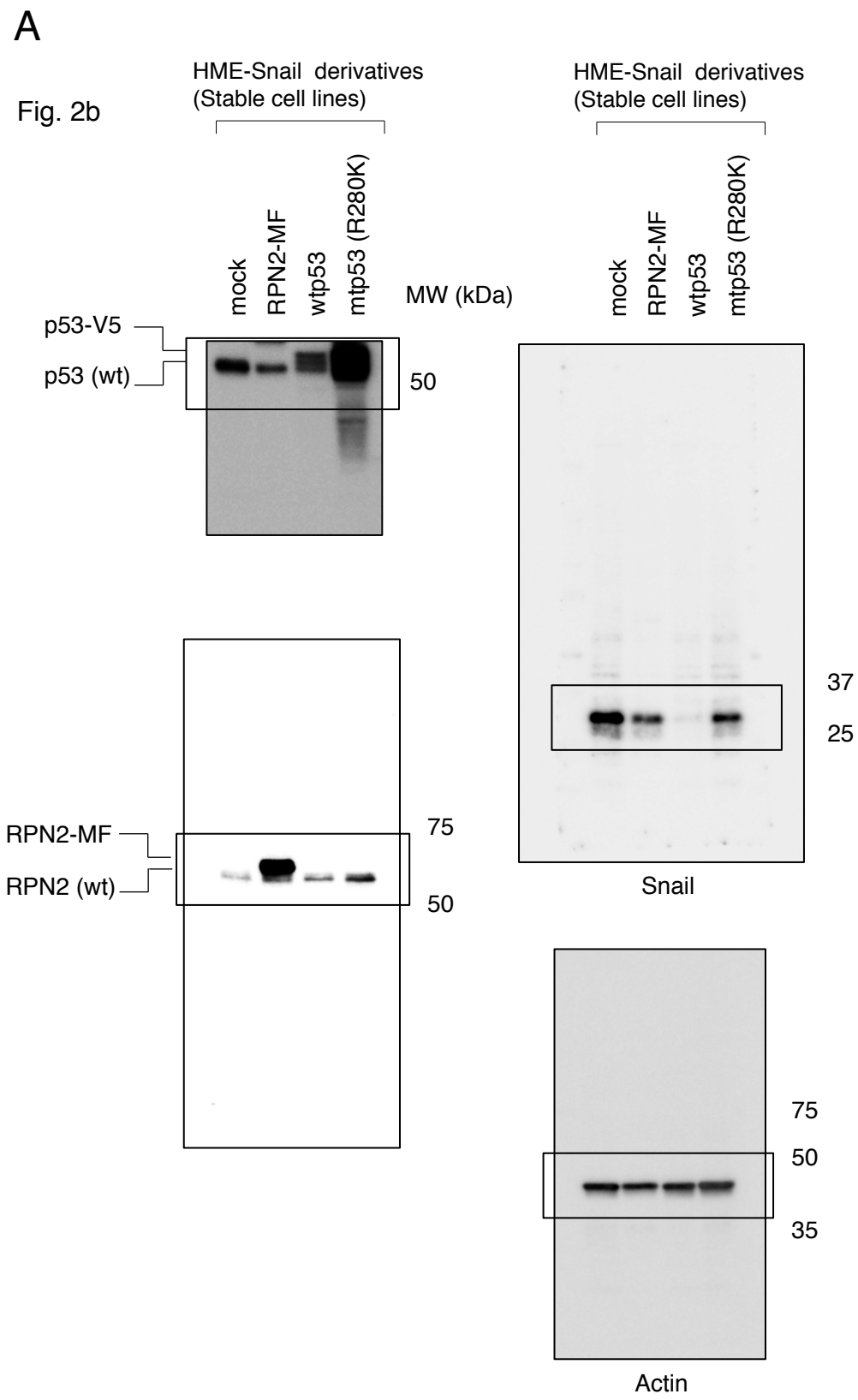

Figure S11 Full scans of western blots shown in the main and supplementary figures. (A) The full blots shown in Fig. 2b.

A

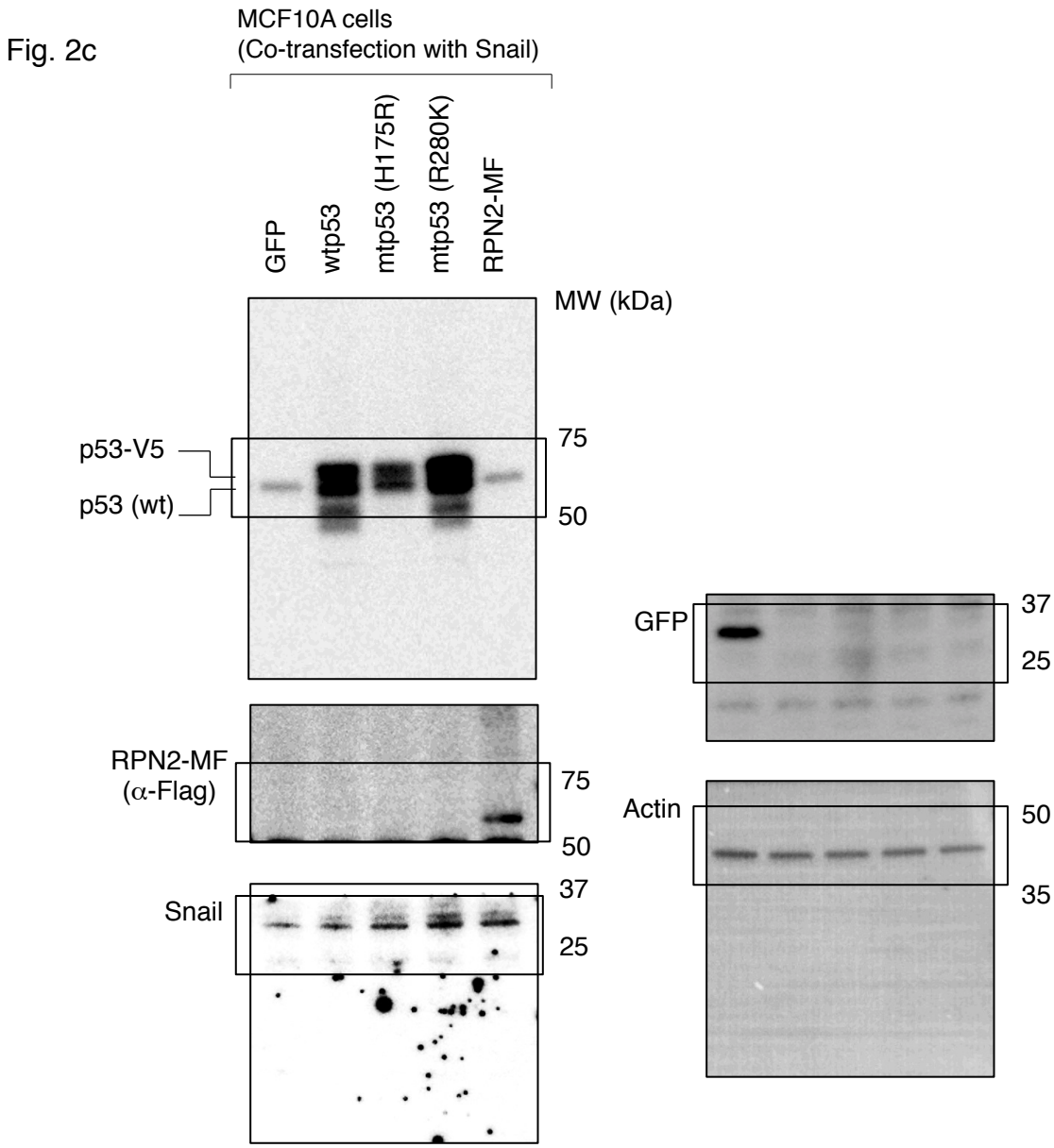

Figure S12 Full scans of western blots shown in the main and supplementary figures. (A) The full blots shown in Fig. 2c.

A

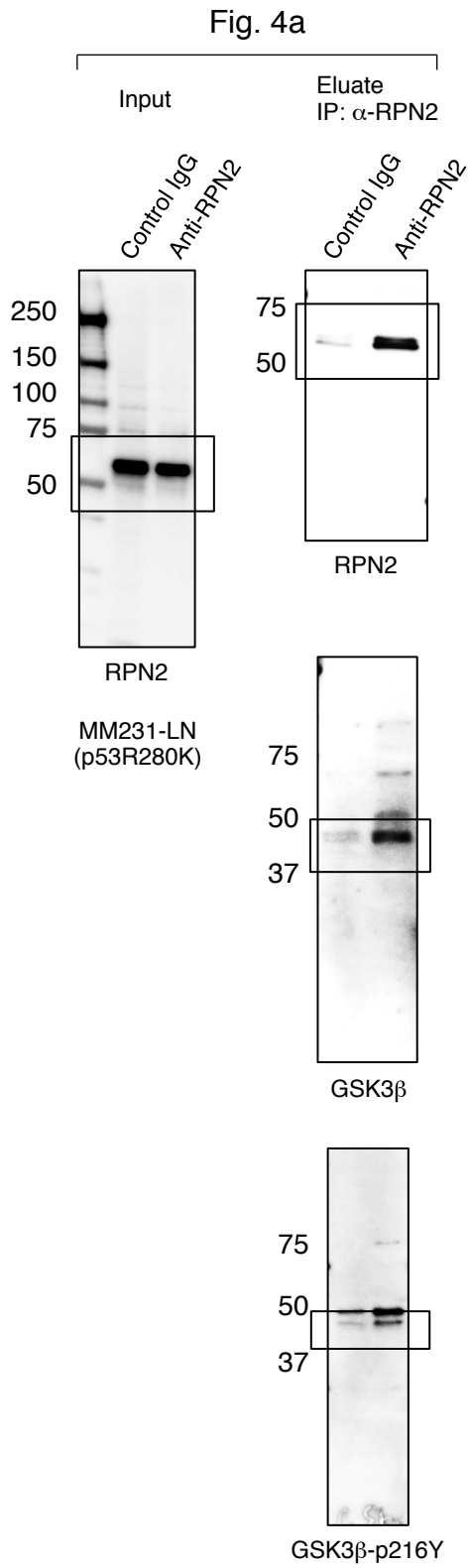

Figure S13 Full scans of western blots shown in the main and supplementary figures. (A) The full blots shown in Fig. 4a.

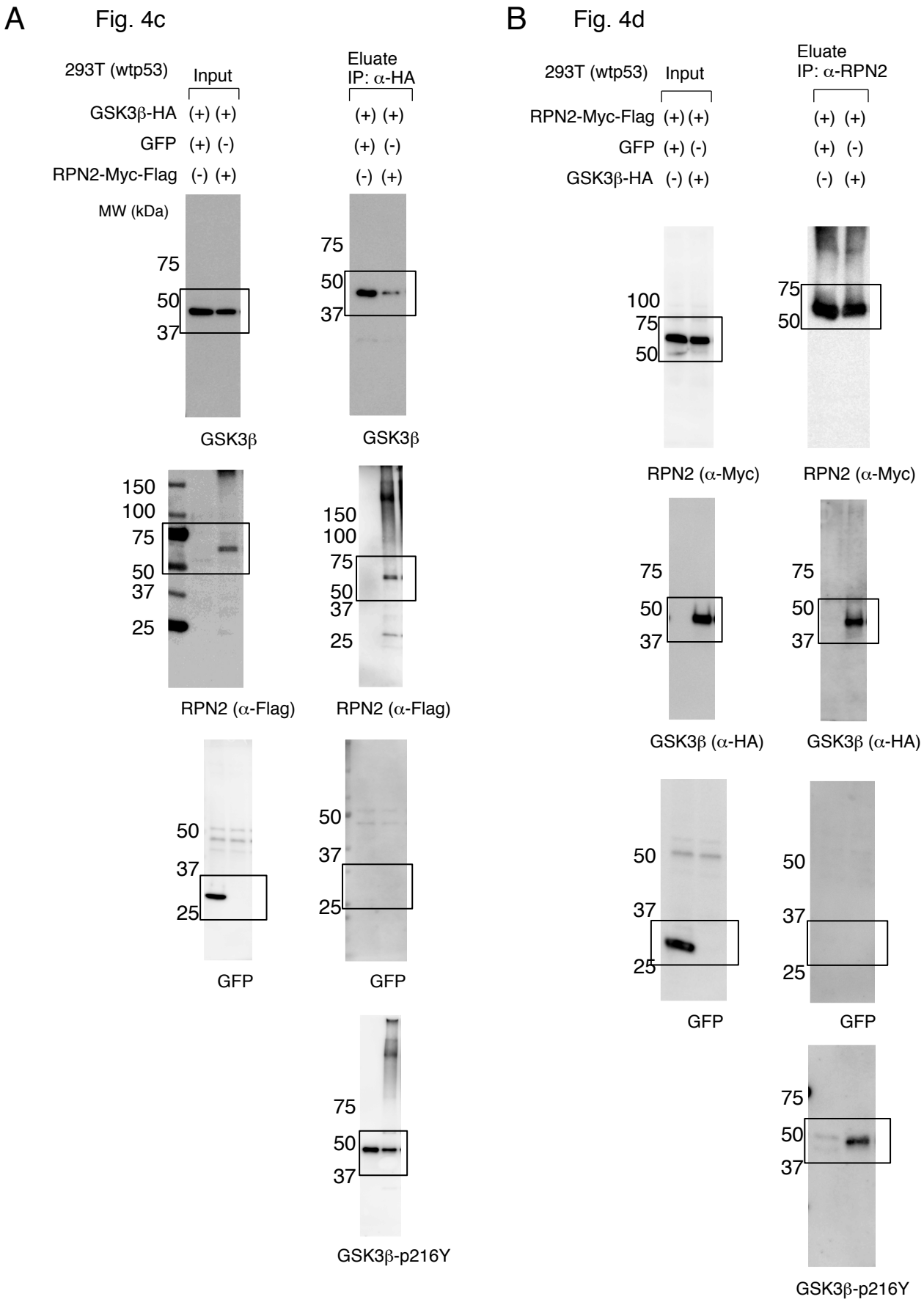

Figure S14 Full scans of western blots shown in the main figures. (A) The full blots shown in Fig. 4c with the locations of MW. (B) The full blots shown in Fig. 4d.

A

Fig. 5a

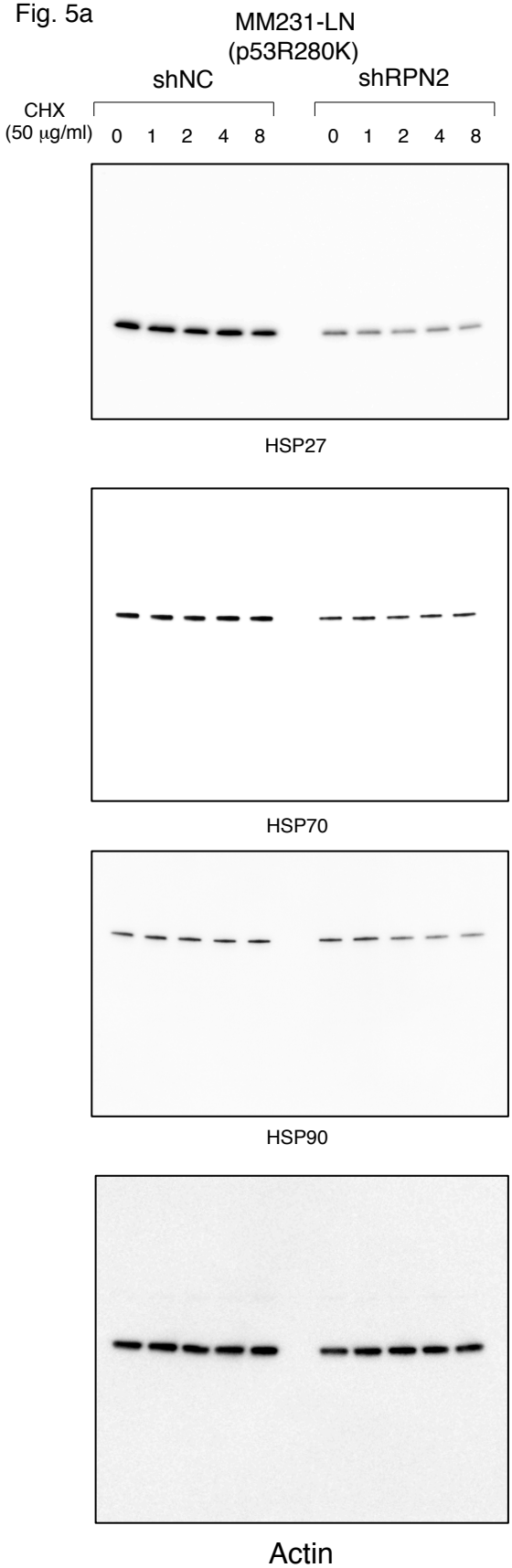

B

Fig. 5b

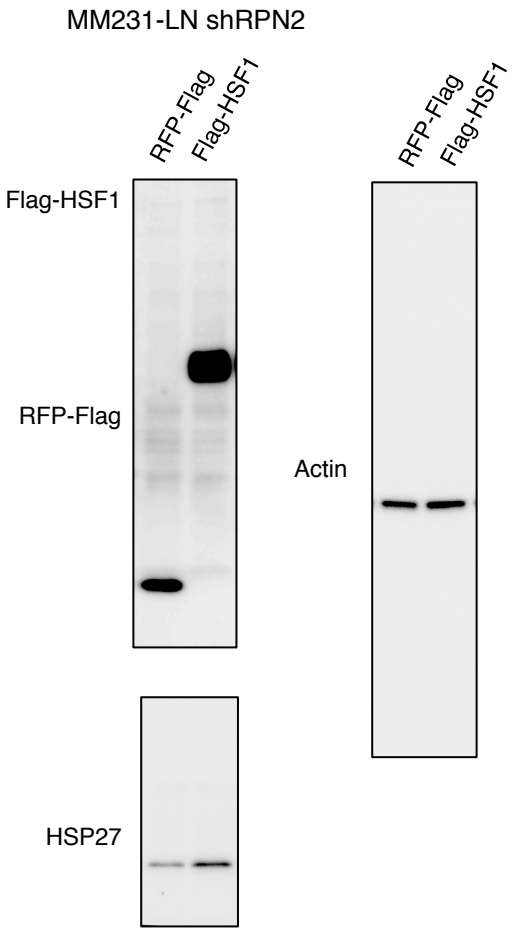

Figure S15 Full scans of western blots shown in the main figures. (A) The full blots shown in Fig. 5a. (B) The full blots shown in Fig. 5b

A

Fig. 6e

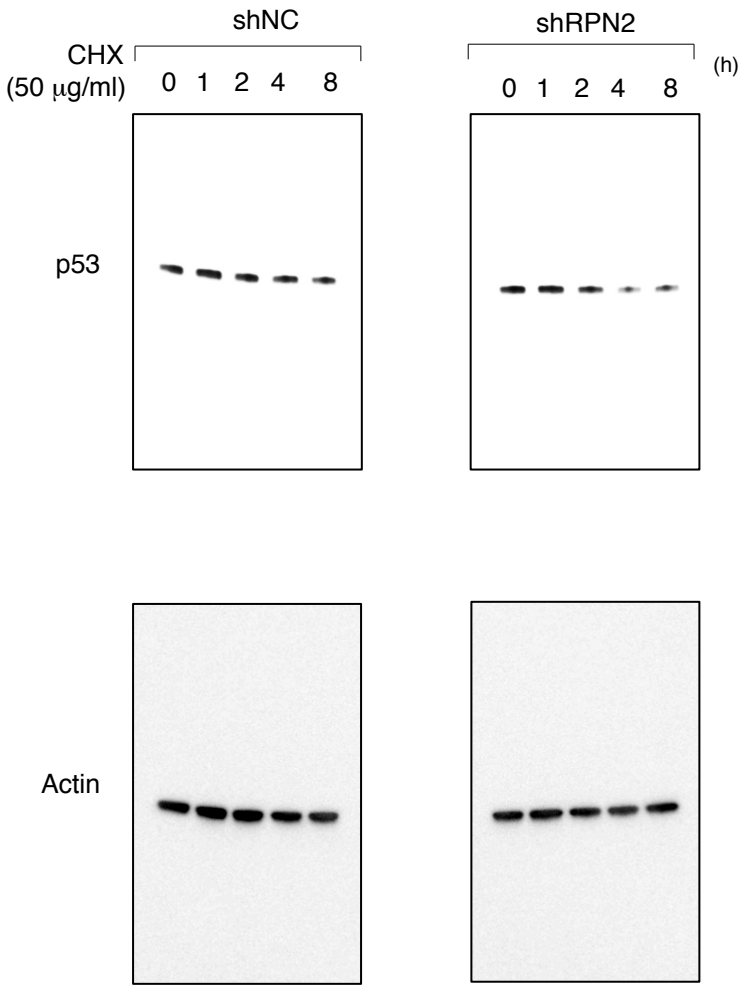

Figure S16 Full scans of western blots shown in the main figures. (A) The full blots shown in Fig. 6e.

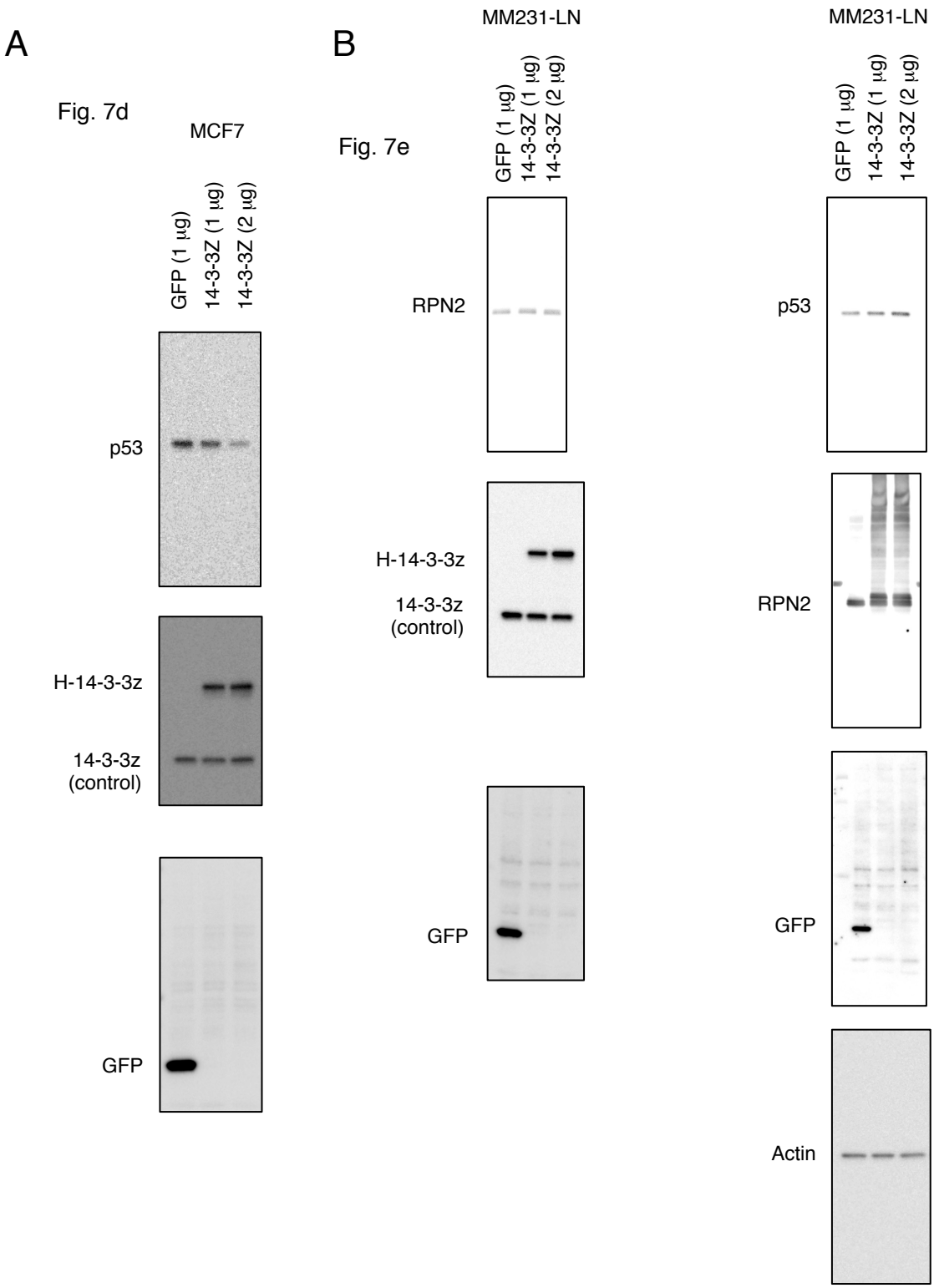

Figure S17 Full scans of western blots shown in the main figures. (A) The full blots shown in Fig. 7d. (B) The full blots shown in Fig. 7e.

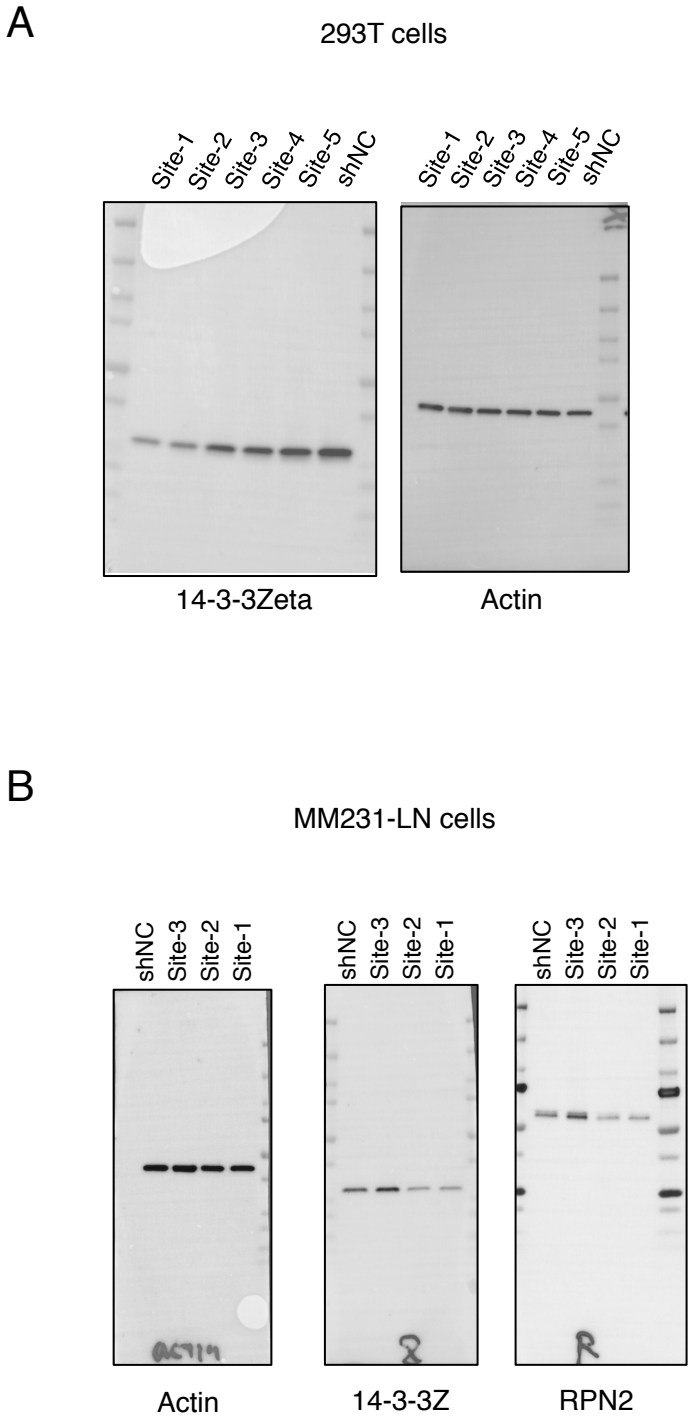

Figure S18 Full scans of western blots shown in the main figures. (A) Knockdown efficacy of lentivirus vectors expressing shRNA against 14-3-3zeta. (B) The full blots shown in Fig. 7h.

Upregulated

ID	RATIO (shRPN2/shNC)	ISCORE	EXPECT	SEQUENCE
1433Z_HUMAN	9.58	33.6	0.058	DSTLIMQLLR
ACTN1_HUMAN	2.95	36.42	0.034	LASDLLEWIR
ACTN4_HUMAN	2.95	36.42	0.034	LASDLLEWIR
RS10_HUMAN	30.61	47.47	0.002	IAIYELLFK
HNRPK_HUMAN	3.68	55.95	3.10E-04	IILDLISESPIK
CLH1_HUMAN	14.49	33.72	0.048	LLLPWLEAR

Downregulated

ID	RATIO (shRPN2/shNC)	ISCORE	EXPECT	SEQUENCE
ISCA2_HUMAN	0.5	30.44	0.13	AVTPWPR
HBB_HUMAN	0.37	36.73	0.027	LLVVYPWTQR
BGAT_HUMAN	0.52	31.34	0.057	VSLPR
MYOZ2_HUMAN	0.52	31.34	0.057	VSIPR
YP023_HUMAN	0.52	31.34	0.057	VSPPR
CQ047_HUMAN	0.52	31.34	0.057	VSPPR
VTNC_HUMAN	0.28	51.98	7.30E-04	DVWGIEGPIDAAFTR
ALBU_HUMAN	0.27	34.99	0.034	YLYEIAR
QSOX1_HUMAN	0.35	32.28	0.079	LAGAPSEDPQFPK
P53_HUMAN	0.35	5.82	35	ALPNNTSSSPQPK

Table S1. Detected peptides that differed between RPN2 knockdown cell line (MM231-LN shRPN2) and control (MM231-LN shNC). Protein identification of peptide peaks with significant difference between MM231-LNshNC and MM231-LN shRPN2.

Table S2. The sequences of primers for real-time RT-PCR analysis

Gene	Forward Primer	Reverse Primer
ACTB	ATTGCCGACAGGATGCAGA	GAGTACTTGCGCTCAGGAGGA
RPN2	CTTCCAGAGCCACTGTCCTC	CCGGTTGTCACCTTCAACTT
p53	TAACAGTTCCTGCATGGGCGGC	AGGACAGGCACAAACACGCACC
SNAIL	ACCCCACATCCTTCTCACTG	TACAAAAACCCACGCAGACA